Surface Diffusion of Underpotential-Deposited Lead Adatoms on Gold Nanoelectrodes

Baodan Zhang, Wei Wang, Cheng Liu, Lianhuan Han, Juan Peng, Alexander Oleinick, Irina Svir, Christian Amatore, Zhong-Qun Tian, Dongping Zhan, et al.

Surface Diffusion of Underpotential-deposited Lead Adatoms on Gold Nanoelectrodes

Baodan Zhang,[a] Wei Wang,*[,a,b] Cheng Liu,[b] Lianhuan Han,[a] Juan Peng,[c] Alexander Oleinick,[d] Irina Svir,[d] Christian Amatore,*[,a,d] Zhong-Qun Tian,[a] Dongping Zhan,*[,a,c]

Dedicated to honor the memory of Prof. Jean-Michel Savéant and to acknowledge his legacy to electrochemical sciences.

a State Key Laboratory of Physical Chemistry of Solid Surfaces; Fujian Science & Technology Innovation Laboratory for Energy Materials of China; Engineering Research Center of Electrochemical Technologies of Ministry of Education; Department of Chemistry, College of Chemistry and Chemical Engineering; Department of Mechanical and Electrical Engineering, School of Aerospace Engineering; Xiamen University, Xiamen 361005, China. E-mail: dpzhan@xmu.edu.cn

b Dr. W. Wang, Dr. C. Liu
College of Chemistry and Chemical Engineering, Jinggangshan University, Ji'an 343009, Jiangxi, China. E-mail: wangwei@jgsu.edu.cn

c Dr. J. Peng, Prof. Dr. D. Zhan
Department of Chemistry, College of Chemistry and Chemical Engineering, Ningxia University, Yinchuan 750021, China.

d Dr. Alexander Oleinick, Prof. Dr. Irina Svir, Prof. Dr. Christian Amatore
PASTEUR, Département de Chimie, École Normale Supérieure, PSL University, Sorbonne Université, CNRS, 24 rue Lhomond, 75005 Paris, France. E-mail: christian.amatore@ens.psl.eu

Abstract: A simple and readily applicable voltammetric approach is described to characterize and measure the site-hopping surface diffusion of underpotential-deposited (UPD) metal adatoms at nanoelectrodes. UPD refers to the deposition of atoms on foreign metal supports at potentials lower than those predicted by Nernst law for a bulk deposition. Despite its importance in several fields of catalysis, advanced nanofabrication or even atomic nanoengineering by atomic layer epitaxy, diffusion of UPD adatoms is difficult to observe at micro- and macroelectrodes. In fact, at electrodes of usual dimensions, UPD adatoms surface diffusion is masked by other electrochemical phenomena of greater relative amplitudes. Conversely, at nanowires electrodes sealed in glass, only an extremely small fraction of the surface of the wires is exposed to the electrolyte solution and is rapidly loaded. This allows the spillage of UPD adatoms onto the much larger area of the nanowire rod which is immune to Faradaic reactions due to its isolation from the electrochemical solution by the glass casing. Therefore, surprisingly for a UPD process, voltammetric peaks currents and integral desorption charges primarily reflect these diffusional surface processes so that the integral charges vary linearly with the inverse of the square root of the scan rate. This is easily observable and measurable with usual bench-level electrochemical instrumentation. In this work, by using nanoelectrodes with diameters between 90 and 260 nm, we were able to establish the major involvement of this site-hopping surface diffusion of UPD Pb adatoms on polycrystalline gold (Au) and characterize it quantitatively. The equivalent surface diffusion coefficient of UPD Pb adatoms was determined to be ~4.4 × 10^{-11} cm^2 s^{-1} at room temperature, corresponding to a Gibbs free energy activation barrier of ca. 18.72 kJ mol^{-1} (i.e., 0.19 eV per Pb adatom) for the reaction of inter-sites exchange of Pb adatoms on a polycrystalline Au surface.

Introduction

UPD refers to the deposition of metal adatoms (M_{ad}) on surface sites of different solid metal supports (S_{sites}) at an energy lower than that corresponding to the equilibrium potential predicted by the Nernst's law for a bulk deposit.[1] This electrochemical phenomenon occurs when M_{ad}-S_{sites} interactions are stronger than M-M_{bulk} ones. Then, the electroreduction of free M cations (or M-containing species) into Mad adatoms on Ssites requires a less negative potential than on metallic M substrate.[2]

Because M and S have different electronic work functions, the valence electron densities of M_{ad}-S_{sites} bonds are not shared equally between the two moieties which therefore carry formal partial charge numbers.[3] For this reason, UPD adatoms may significantly modulate the catalytic and electrocatalytic properties of their metal supports

by affecting their geometric and/or electronic structure or their surface energy. This makes them prone to play crucial roles in electrocatalysis,[4] as well as in heterogeneous catalysis (where this phenomenon is often referred to as “electron spilling” or “support effect”).[5] For example, UPD adatoms can inhibit catalyst poisoning, and may drive a reaction selectively towards a particular product,[6] or provide adsorption sites for reactive species to facilitate bifunctional catalysis.[7] Interestingly, all these effects can be finely tuned to define the ultimate properties of (electro)catalysts by taking advantage of the fact that the coverage of a substrate by UPD adatoms is generally easily controllable.[8] It should be noted in this regard that since the maximum UPD coverage of a metal substrate is necessarily limited to the formation of a monolayer of adatoms, the electrochemical charge associated to the stripping of UPD adatoms can be used effectively to determine the “real” surface area of metal catalysts.[9]

UPD is also important in controlling nucleation and growth during subsequent electrodeposition processes.[10] For example, it can be used to form seed-layers to improve the quality of electroplating by controlling the binding strength between a substrate and additional plating layers.[11] This principle can even be extended to allow layer-by-layer nanoengineering of crystalline and polycrystalline materials in controlled atomic layer epitaxy (ALE). [12] For example, such an electrochemical atomic layer epitaxy (EC-ALE) has been designed to nanofabricate nanofilm of CdTe semiconductor on Au(111) by alternating electrodeposition of Cd and Te atomic layers.[13] Finally, UPD metals can even be used to load non-UPD metals onto a nanostructure by resorting to replacement reactions to form core-shell nanostructures.[14] Hence, provided that all its dynamic are fully mastered at the atomic level, UPD should play an increasing role in nanofabrication or even atomic fabrications.[15]

However, the observation of clusters forming by aggregation of UPD adatoms demonstrates the existence of their surface diffusion and the way in which this can alter the desired properties of the overall material.[16] A proper understanding and a quantitative characterization of the surface diffusion of UPD adatoms is therefore crucial for the success of most of the above applications. However, investigating surface diffusion of UPD adatoms is extremely difficult experimentally[17] unlike what can be done for nucleation processes during overpotential deposition (OPD).

Hereafter, we wish to validate the extreme efficiency of a simple electrochemical strategy allowing such precise investigations. At usual electrodes, surface diffusion of adatoms is masked by the greater relative magnitude of the combined effects of heterogeneous Faradaic reactions and resulting transport processes occurring in the electrolyte. Conversely, at sealed nanodisk electrodes, only a very small fraction of the surface of the metallic nanowires is exposed to the electrolyte solution and is expected to be rapidly loaded or unloaded leading to classical bell-shaped voltammograms as occurs at larger electrodes. Nonetheless, we report thereafter that in the case of UPD lead adatoms deposited on polycrystalline Au nanodisk electrodes, the Pb UPD process can extend far beyond the expected full coverage of the nanodisk surface. This is shown to be due to the spillage of UPD lead adatoms across the nanodisk edge and their ensuing site-hopping diffusion onto the cylindrical surface of the nanowire rod which is isolated from the solution by its glass casing. This phenomenon provides a simple bench-level voltammetric method for energetically and kinetically characterizing the site-hopping surface diffusion of UPD lead adatoms onto polycrystalline Au.

Results and Discussion

Polycrystalline Au disk nanoelectrodes were prepared with a laser puller and polished by a precision sander to expose Au nanodisks as reported previously by some of us.[18] Ferrocenemethanol (FcMeOH) was adopted as the redox couple to characterize the apparent geometric size of the corresponding Au nanodisk electrodes, because its redox reaction involves a simple electron transfer mechanism and follows a well characterized diffusion-limited mass-transfer process with a diffusion coefficient of 7.8 × 10-6 cm^2 s^{-1} for FcMeOH in 0.1 M K2SO4.[19] Also, and more importantly for our objective in this work, an outer-sphere electron-transfer reaction would take place in this system, not involving sensible Faradaic adsorption. Accordingly, the well-defined steady-state cyclic voltammograms were obtained as typified in Fig. 1a. From the steady-state limiting current in Fig. 1a, an apparent diameter of 96 nm was determined for the examined Au nanodisk electrode. The diameters of all others nanodisk

electrodes used in this study were determined by the same method and ranged between 90 and 260 nm (see, e.g., the insets in Figs. 2a-c).

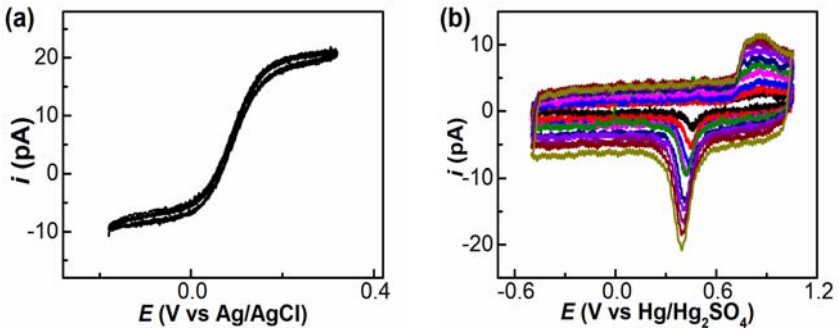

Figure 1. (a) Steady state voltammogram recorded at a 96 nm diameter Au nanodisk electrode in an aqueous solution containing 1 mM FcMeOH and 0.1 M K_2SO_4 at a scan rate of 0.1 V s^{-1} (b) Cyclic voltammograms recorded at the same Au nanodisk electrode in an aqueous solution containing 0.5 M H_2SO_4 for a series of 10 scan rates (from smallest to largest CV: v = 0.1 V s^{-1} to 1 V s^{-1} increasing in steps of 0.1 V s^{-1}), T = 25°C.

Before any UPD experiment, the Au nanoelectrodes surfaces were cleaned, pretreated and activated by repetitive voltammetric cycling in 0.5 M H2SO4 solution saturated by nitrogen gas.[20] Classical voltammetric behaviors of polycrystalline Au electrode in H2SO4 were observed (Fig. 1b) denoting a clean and homogenous Au surface, where the faraday currents of water-dissociation adsorption (anodic scan) and the oxygen-adspieces desorption (cathodic scan) were well-defined as those obtained on macro- and micro-electrodes.[21]

Figs. 2a-c report a series of cyclic voltammograms recorded for UPD of Pb on polycrystalline Au at three different Au nanodisk electrodes at a series of scan rates increasing from 0.1 V s^{-1} to 1 V s^{-1} in steps of 0.1 V s^{-1}. The inserts are the steady-state voltammograms of each nanoelectrode obtained with the same experimental conditions as described in Fig. 1a, which are employed to determine the apparent diameter of each nanoelectrodes. As it is classically obtained at Au macroelectrodes, two cathodic UPD waves were observed around at -0.55 V and -0.68 V, and two anodic stripping waves were observed around at -0.65 V and -0.38 V vs. a Hg/Hg_2SO_4 reference electrode with a scan rate of 0.1 V s^{-1}.[22] The redox peaks at (-0.68 V, -0.65 V) were assigned to the UPD Pb on Au(111) facet, and the redox peaks at (-0.55 V, -0.38 V) were assigned to the UPD Pb on Au(100) and Au(110) facets which may involve some surface reconstruction. That the potential differences of the corresponding current peaks are pretty larger than those observed at conventional Au macroelectrodes, may predict some unique behavior at Au nanoelectrode.

However, unlike with larger Au electrodes,[22,23] the charge associated with the stripping of UPD Pb adatoms was found to increase in proportion to the inverse of the square root of the scan rates (Figs. 2d-f). It should be noted that, since in our experiments the concentration of Pb^{2+} is as high as 1 mM, the mass flux should be enough for the UPD reaction occurring at the Au nanodisc electrode/solution interface. On the Au macroelectrode, the current should be in proportion to the scan rate. This apparently strange behavior is nevertheless in full agreement with what some of us have already observed when studying the surface electrochemistry of platinum nanoelectrodes in sulfuric acid.[18] As previously rationalized in these previous works, this rare behavior for stripping voltammetric waves results directly from the nanometric sizes of current Au nanowires. Indeed, at a given potential, comparing with macroelectrodes, the complete loading of the extremely small surface area of the Au nanodisks that is exposed to the electrolyte solution with UPD Pb adatoms corresponds to a very low charge consumption. UPD Pb adatoms can then spill over the edge of the nanodisks and accumulate in relatively larger quantities through site-hopping propagation onto the rod surface of the nanowires as sketched in Figure 3. This latter process, equivalent to diffusion,[24] is invisible at larger usual electrodes since the UPD atoms ultimately present on the disk electrode area are then stored in much larger quantities relative to those which can spill over onto the nanowire rod due to the small values of site-hopping diffusion coefficients (see below). Yet, it becomes the dominant one that controls the Faradaic processes at nanoelectrodes. We also observed the peak potentials

for the UPD and stripping processes shift with the scan rate. This quasi-reversible behavior is indeed caused by the Gibbs free energy of the surface diffusion of the UPD Pb adatoms on Au surface, which will be quantified later by the temperature-controlled experiments.

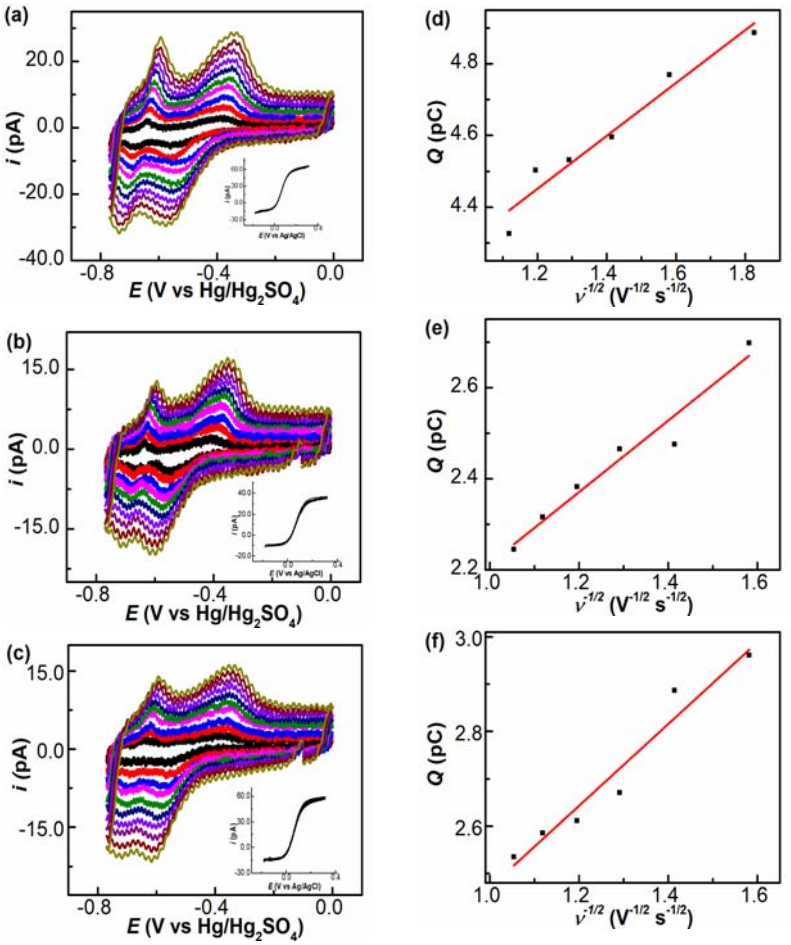

Figure 2. (a-c) Cyclic voltammograms recorded at three Au nanodisk electrodes (diameters: (a) 257 nm, (b) 182 nm, (c) 239 nm) in an aqueous solution containing 1 mM $Pb(NO_3)_2$ and 0.1 M $NaClO_4$ at a series of 10 scan rates in each case (from smallest to largest CV: 0.1 V s^{-1} to 1 V s^{-1} by increments of 0.1 V s^{-1}). The inset in each panel reports the steady-state voltammogram recorded at the same Au nanodisk electrode in an aqueous solution containing 1 mM FcMeOH and 0.1 M K_2SO_4 at a scan rate of 0.1 V s^{-1} (compare Fig. 1a). (d-f) Linear relationship between the integral desorption charge of UPD Pb adatoms and the inverse of the square root of scan rates corresponding to the voltammograms in (a-c) respectively. *T* = 25°C.

Hence, at sufficiently small nanoelectrodes, the UPD Pb stripping current, i, and the corresponding stripping charge, Q, are essentially representative of the quantities of UPD Pb adatoms that were stored over the nanowire rod surface. Indeed, both i and Q vary with the square-root of the scan rate, $v^{1/2}$, as occurs for classical linear diffusion processes, and no component proportional to the scan rate, v, as usually expected for a capacitive contribution or for the stripping of a fixed quantity of UPD Pb adatoms adsorbed on the nanodisk Au surface.[25a,b] Note that the absence of any capacitive component is perfectly normal for nanodisks of a few hundreds of a nanometer or less in the range of scan rates investigated here (compare Fig. 1a). In other words, this result implies that the quantity of UPD Pb adatoms that diffused and adsorbed by site-hopping sequences[24] along the rod flank surface of the nanowire during one voltammetric scan largely exceeds that adsorbed over the nanodisk exposed to the solution.[25c] Note indeed that the UPD Pb monolayer surface concentration on the Au nanodisk electrode surface area exposed to the solution must obey a near steady-state regime at each instant owing to the extremely small time constant, $\theta_{dif} = r_{disk}^2/2D_{soln}$, of diffusional transport from the solution to the nanodisk surface where r_{disk} is the radius of the Au nanowire, and D_{soln} the diffusion coefficient of Pb(II) species in the solution. $C_{\mathrm{UPD\,Pb}}^{\mathrm{disk}}$ has

therefore to keep its saturation value, $C^{sat}_{UPD\ Pb}$, i.e., 305 μC cm^{-2} symbolized as C* in following Eq. (1),[22a] while UPD Pb adatoms spill over the nanowire rod flank. Accordingly, the stripping charge may be expressed as in Eq. (1)[18a,25]

$$Q = \int_{E_2}^{E_1} i\,dt = nFDC^*(2\pi r_{disk})\left[\int_{E_2}^{E_1}\chi(\sigma t)\,dE\right]\left(\frac{\pi nF}{DRT}\right)^{1/2} v^{-1/2} \quad (1)$$

where, D is the equivalent surface diffusion coefficient of UPD Pb site-hopping,[24] E1 and E2 the initial and final desorption potentials of UPD Pb, R the perfect gas constant, T the temperature, and $\chi(\sigma t)$ is the canonical function introduced by Nicholson and Shain. The validity of the above assumptions justifying the use of Eq. (1) to account for the stripping charge[25c] are confirmed *a posteriori* by the fact that the time constant of diffusional transport from the solution to the nanodisk surface, θ_{dif}, is effectively much smaller than that, $\theta_{CV} = DRT/(nFv)$, of the linear diffusion of the adatoms along the Au nanowire shaft imposed by the voltammetric scan rates. Indeed, based on a series of experiments performed using several nanowire disk electrodes (see, e.g., Fig. 2), the surface diffusion coefficient of UPD Pb (D) was evaluated to be 4.4 × 10-11 cm^2 s^{-1} at 25 C°. This value is in fair agreement with a previous experimental estimation based on low energy electron diffraction (LEED), from which the half mean distance of atomic steps on Au was evaluated as 20 nm. [22b]

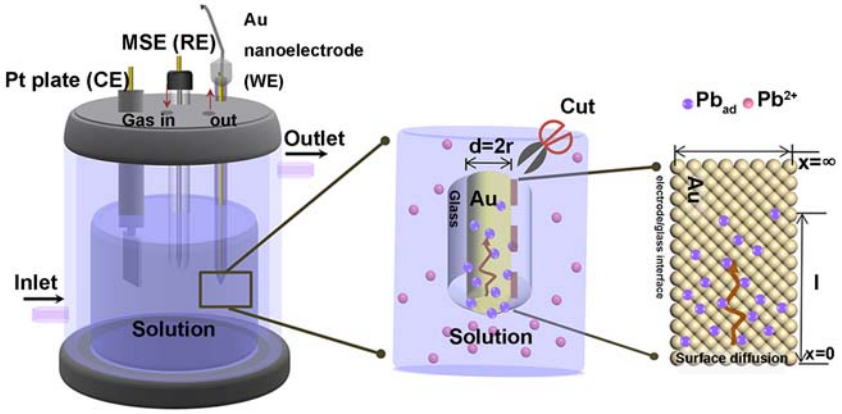

Figure 3. Left: Schematic representation of the double-jacket electrochemical 3-electrode cell used in this work. Center: Close-up cartoon of the tip of one of the Au nanoelectrodes placed in the 1 mM $Pb(NO_3)_2$ and 0.1 M $NaClO_4$ thermostated bulk solution. Right: Sketch of the site-hopping equivalent linear diffusion of UPD Pb adatoms onto the Au surface of the microwire shaft (the surface is "unfolded" so that shat-disk edge contact is shown as the bottom boundary over which UPD Pb adatoms are spilling when the nanodisk surface area exposed to the solution is fully loaded; Au atoms are represented by the array of solid yellow circles in the right cartoon).

An empirical Arrhenius equation is often adopted to investigate kinetic properties of surface diffusion [24c-f]:

$$D = D_0 \exp[-\Delta E_d/kT] \quad (1)$$

where, D_0 is a pre-exponential factor, ΔE_d the activation energy of site-hopping reactions,[24b] k the Plank constant, and T the absolute temperature. From the linear relationship observed between lnD and 1/T (see Fig. 4f), one obtains D_0 = 1.1 × 10-6 cm^2 s^{-1} and ΔEd = 0.19 eV (i.e., 18.72 kJ mol^{-1}).

Indeed, when an electrode size is reduced to nanometric scales, the relative amplitudes of the contributions of the classical phenomena of solution diffusion and Faradaic adsorption / desorption, which remain linked to the surface area of the nanodisk exposed to the solution, and that of the diffusion of adatoms along the nanowire rod of much larger surface area is reversed compared to what occurs with larger electrodes. At usual macro- or microdisks electrodes, there is essentially an involvement of charge transfers reactions coupled to diffusion of electroactive species in the solution and with the loading/unloading of UPD adatoms onto the microdisk surface area exposed to the solution. This combination of phenomena conventionally considered when it comes to large usual electrodes underlies the observation of sharp bells conventionally expected for stripping voltammetric waves. On the contrary, as soon as the size of a nanoelectrode is sufficiently small, one can observe the comparatively more important spillage of the UPD adatoms over the edge of the electroactive disc exposed to the electrolyte and

their subsequent diffusion by site hopping along the atomic surface of the metallic substrate of the rod hidden from the solution by its glass casing. Indeed, due to the low magnitudes of the equivalent diffusion coefficients that is imposed by the values of activation barriers of the UPD Pb site exchange reactions onto the Au surface, this spilling phenomenon may become visible and ultimately dominates the whole electrochemical behavior only for electrodes constructed from nanowires of a few hundred nanometers or less. It is then observed that the voltammetric waves featuring the UPD loading and unloading of Pb adatoms on polycrystalline Au exhibit classical diffusional shapes and that the integral charges corresponding to the UPD Pb stripping waves vary proportionally to the inverse of the square root of the voltammetric scan rate, revealing that that surface site-hopping diffusion is the rate-determining step of the global UPD Pb process on the Au nanoelectrode.

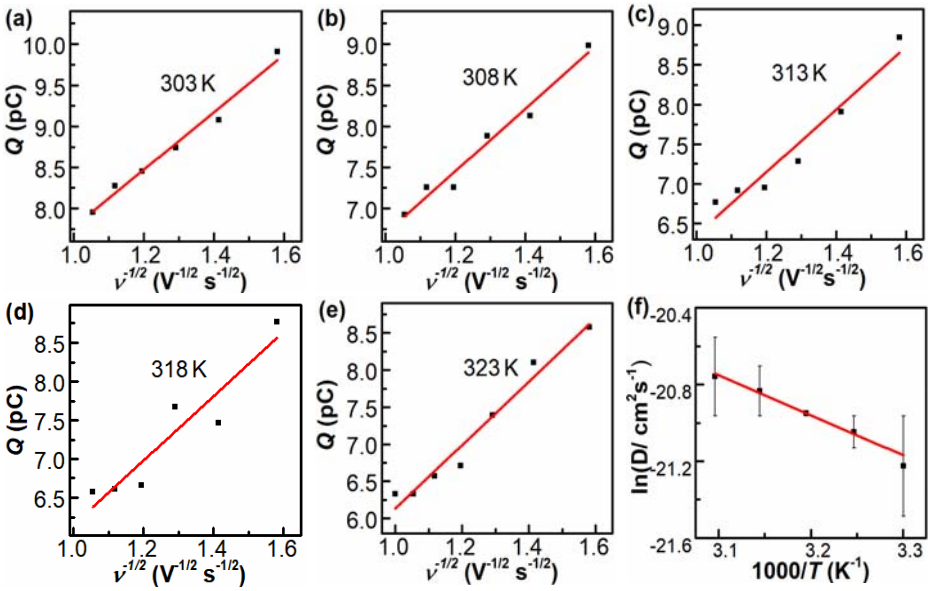

Figure 4. (a-e) Linear correlations between the integral desorption charge of UPD Pb adatoms and the reciprocal of the square root of scan rate at different temperatures as indicated in each panel. (f) Arrhenius plot for the variations of the natural logarithm of the apparent surface diffusion coefficient values *D* of UPD Pb adatoms with the reciprocal of the temperature. All data were recorded at a 286-nm-diameter Au disc nanoelectrode in an aqueous solution containing 1 mM $Pb(NO_3)_2$ and 0.1 M $NaClO_4$ at a series of 10 scan rates in each case (from smallest to largest CV: 0.1 V s^{-1} to 1 V s^{-1} by increments of 0.1 V s^{-1}).

Conclusion

The underpotential deposition of Pb on polycrystalline Au surface has been reexamined taking advantage of nanodisk electrodes special features associated with their extremely small sizes, as this provides new and easy access to measurements of surface diffusion of UPD Pb adatoms on polycrystalline Au with usual bench-level cyclic voltammetry. Taking advantage of this unique behavior, using simple voltammetric experiments, the apparent surface diffusion coefficient of UPD Pb adatoms on polycrystalline Au surface could be determined to be ~4.4 × 10^{-11} cm^2 s^{-1} (at 25 C°) corresponding to an activation energy barrier of 18.72 kJ mol^{-1}. We believe that this simple and practical methodology based on classical voltammetric experiments performed at nanodisk electrodes will not only prove significant for kinetic investigations related to electroplating processes, but will also present several interesting applications in the sciences of nanoengineering. For example, this approach can certainly be used with great interest, especially in the fields of electrocatalysis, nanofabrication and electrochemically driven atomic-layer epitaxy, but also for the design of better heterogeneous catalysts due to the importance of surface diffusion of adatoms during the formation of reactive metal clusters and/or for preventing their inactivation due to their uncontrolled growth.

Experimental Section

Chemicals and materials

Ferrocenemethanol ($C_{11}H_{12}FeO$, 99%) were purchased from Alfa Aesar, sulfuric acid (H_2SO_4), hydrogen peroxide (H_2O_2), lead nitrate ($Pb(NO_3)_2$), potassium sulfate (K_2SO_4) and sodium perchlorate ($NaClO_4$) were provided by Sinopharm Group Co. Ltd and used without further purification. Aqueous solutions were prepared from deionized water (18.2 MΩ•cm, Milli-Q, Millipore,Co).

Preparation of Au disc nanoelectrodes

All Au disc nanoelectrodes used in experiment were fabricated by a laser-beam heating puller (P-2000,Sutter Co., USA).[18] A 25-μm-diameter Au wire was pulled inside a borosilicate glass capillary (Drummond Co. USA; 1.0 mm o.d., 0.2 mm i.d.). With a programmed laser puller, the middle part of the capillary was pre-thinned, and the Au wire was then sealed into the capillary under vacuum with the second heating process. The sealed part of capillary was heated, pulled and broken into two almost identical parts during heating process. After that, a 100-μm-diameter Ni wire was inserted into the capillary as electrical connector. Finally, the nanoelectrode tip was polished using a Sutter BV-10 beveller (Sutter Co., USA).

Electrochemical Measurements

Electrochemical experiments involving the Au nanodisk electrodes were performed with a Autolab workstation (PGSTAT302NC, Metrohm Autolab Co., Netherlands) in a three-electrode thermostatically controlled cell installed inside a Faraday cage at room temperature (298 K) unless stated otherwise. Solutions were purged by bubbling high-purity argon to remove the dissolved oxygen in experiments.

To determine the apparent geometric size of each Au nanodisk electrode, steady-state voltammograms were recorded in an aqueous solution containing 1 mM Ferrocenemethanol and 0.1 M K_2SO_4 at a scan rate of 0.1 V s^{-1}, with Ag/AgCl wires used as reference and counter electrodes.

Cyclic voltammetry in an aqueous solution containing 0.5 M H_2SO_4 was performed to judge of the surface status of the Au disc nanoelectrodes (leakage, cleanliness, electric double layer, etc.). In these experiments, a Pt plate was used as the counter electrode and Hg/Hg_2SO_4 (MSE) as the reference electrode in order to avoid the interference of Cl- ions (EMSE = 0.64V vs. RHE).

To determine the surface diffusion coefficient of UPD Pb on Au surface, cyclic voltammetry was performed at different scan rates using the electrochemically cleaned Au disc nanoelectrode in an aqueous solution containing 1 mM $Pb(NO_3)_2$ and 0.1 M NaClO4. In order to determine the parameters of the Arrhenius equation (D_0 and ΔEd, in Eq.2) characterizing the site-exchange apparent diffusion coefficient of UPD Pb adatoms onto the polycrystalline Au surface, these experiments were carried out at temperatures ranging from 303 K to 323 K at an interval of 5 K, by connecting the three-electrode thermostatically controlled cell to a continuous flow cryostat (Fig. 3).

Acknowledgements

In China, the financial support of the National Natural Science Foundation of China (21802057, 21827802 and 22021001), the Jiangxi Education Department (GJJ190571), the Fundamental Research Funds for the Central Universities (20720190023) are appreciated by all co-authors. In Paris, this work was supported in parts by CNRS, ENS-PSL University and Sorbonne University (UMR 8640 PASTEUR). All co-authors from Xiamen and Paris groups greatly acknowledge the Sino-French LIA CNRS NanoBioCatEchem for supporting the collaboration between the two teams. All co-authors declare no competing financial interests.

Keywords: under potential deposition • Faradaic adsorption • surface diffusion • nanoelectrode • cyclic voltammetry

References:

[1] a) G. Kokkinidis, *J. Electroanal. Chem.* **1986**, *201*, 217-236; b) O. A. Oviedo, P. Velez, V. A. Macagno, E. P. M. Leiva, *Surf. Sci.* **2015**, *631*, 23-34; c) I. M. Ritchie, S. Bailey, R. Woods, *Adv. Colloid Interface Sci.* **1999**, *80*, 183-231; d) V. Sudha, M. V. Sangaranarayanan, *J. Phys. Chem. B* **2002**, *106*, 2699-2707.

[2] a) C. G. Sanchez, E. P. M. Leiva, J. Kohanoff, *Langmuir* **2001**, *17*, 2219-2227; b) S. Swathirajan, S. Bruckenstein, *Electrochim. Acta* **1983**, *28*, 865-877.

[3] a) M. Chatenet, *Electrocatalysis* **2015**, *6*, 382-389; b) M. Chatenet, Y. Soldo-Olivier, E. Chainet, R. Faure, *Electrochem. Commun.* **2007**, *9*, 1463-1468; c) S. Swathirajan, S. Bruckenstein, *J. Electrochem. Soc.* **1982**, *129*, 1202-1210.

[4] a) M. Chatenet, Y. Soldo-Olivier, E. Chainet, R. Faure, *Electrochim. Acta* **2007**, *53*, 369-376; b) G. Salie, *J. Electroanal. Chem.* **1988**, *245*, 1-20; c) G. Salie, K. Bartels, *J. Electroanal. Chem.* **1988**, *245*, 21-38.

[5] L. Liu, A. Corma, *Chem. Rev.* **2018**, *118*, 10, 4981–5079.

[6] S. Hebie, T. W. Napporn, K. B. Kokoh, *Electrocatalysis* **2017**, *8*, 67-73.

[7] R. R. Adzic, A. V. Tripkovic, N. M. Markovic, *J. Electroanal. Chem.* **1980**, *114*, 37-51.

[8] a) M. R. Langille, M. L. Personick, J. Zhang, C. A. Mirkin, *J. Am. Chem. Soc.* **2012**, *134*, 14542-14554; b) A. Mehere, N. B. Chaure, *Appl. Phys. A* **2020**, *126*, 662; c) F. B. Nisanci, T. Oznuluer, U. Demir, *Electrochim. Acta* **2013**, *108*, 281-287.

[9] a) J. Hernandez, J. Solla-Gullon, E. Herrero, A. Aldaz, J. M. Feliu, *J. Phys. Chem. B* **2005**, *109*, 12651-12654; b) C. Jeyabharathi, M. Zander, F. Scholz, *J. Electroanal. Chem.* **2018**, *819*, 159-162; c) M. Lukaszewski, M. Soszko, A. Czerwinski, *Int. J. Electrochem. Sci.* **2016**, *11*, 4442-4469; d) N. Mayet, K. Servat, K. B. Kokoh, T. W. Napporn, *Surfaces* **2019**, *2*, 257-276; e) N. Mayet, K. Servat, K. B. Kokoh, T. W. Napporn, *Electrocatalysis* **2021**, *12*, 26-35.

[10] a) K. Juttner, W. J. Lorenz, *Zeitschrift Fur Physikalische Chemie-Wiesbaden* **1980**, *122*, 163-185; b) L. H. Mendoza-Huizar, J. Robles, M. Palomar-Pardave, *J. Electroanal. Chem.* **2003**, *545*, 39-45; c) M. Palomar-Pardave, I. Gonzalez, N. Batina, *J. Phys. Chem. B* **2000**, *104*, 3545-3555.

[11] a) W. R. Pitner, C. L. Hussey, *J. Electrochem. Soc.* **1997**, *144*, 3095-3103; b) D. Wu, D. J. Solanki, A. Joi, Y. Dordi, N. Dole, D. Litvnov, S. R. Brankovic, *J. Electrochem. Soc.* **2018**, *166*, D3013-D3021.

[12] a) S. Lin, X. Shi, X. Zhang, H. Kou, C. Wang, *Appl. Surf. Sci.* **2010**, *256*, 4365-4369; b) B. I. Podlovchenko, T. D. Gladysheva, Y. M. Maksimov, D. S. Volkov, K. I. Maslakov, *J. Solid State Electrochem.* **2020**, *24*, 1439-1444; c) T. Suntola, *Mat. Sc. Reports* **1989**, *4*, 261-312.

[13] K. Varazo, M. D. Lay, T. A. Sorenson, J. L. Stickney, *J. Electroanal. Chem.* **2002**, *522*, 104-114.

[14] a) M. Fayette, Y. Liu, D. Bertrand, J. Nutariya, N. Vasiljevic, N. Dimitrov, *Langmuir* **2011**, *27*, 5650-5658; b) I. Mahesh, A. Sarkar, *Electrocatalysis* **2021**; c) Y.-F. Xing, Y. Zhou, Y.-B. Sun, C. Chi, Y. Shi, F.-B. Wang, X.-H. Xia, *J. Electroanal. Chem.* **2020**, *872*, 114348.

[15] a) Z. Y. Aydin, S. Abaci, *Solid State Sci.* **2017**, *74*, 74-87; b) Y. Shi, W.-M. Huang, J. Li, Y. Zhou, Z.-Q. Li, Y.-C. Yin, X.-H. Xia, *Nat. Commun.* **2020**, *11*, 4558-4558.

[16] a) A. Kapoor, R. T. Yang, C. Wong, *Catal. Rev.: Sci. Eng.* **1989**, *31*, 129-214; b) S. Szabo, *Int. Rev. Phys. Chem.* **1991**, *10*, 207-248; c) G. Antczak, G. Ehrlich, *Surface Diffusion: Metals, Metal Atoms, and Clusters* **2010**, 1-757.

[17] a) Y. Liu, S. Bliznakov, N. Dimitrov, *J. Phys. Chem. C* **2009**, *113*, 12362-12372; b) A. Surrey, D. Pohl, L. Schultz, B. Rellinghaus, *Nano Lett.* **2012**, *12*, 6071-6077; c) X. Z. Yao, Y. P. Wei, Z. X. Wang, L. Gan, *ACS*

Catal. **2020**, *10*, 7381-7388.

[18] a) W. Wang, J. Zhang, F. F. Wang, B. W. Mao, D. P. Zhan, Z. Q. Tian, *J. Am. Chem. Soc.* **2016**, *138*, 9057-9060; b) D. P. Zhan, J. Velmurugan, M. V. Mirkin, *J. Am. Chem. Soc.* **2009**, *131*, 14756-14760.

[19] P. Sun, M. V. Mirkin, *Anal. Chem.* **2006**, *78*, 6526-6534.

[20] C. Amatore, J.-M. Savéant, D. Tessier, *J. Electroanal. Chem.* **1983**, *146*, 37-45.

[21] a) S. Cherevko, A. R. Zeradjanin, G. P. Keeley, K. J. J. Mayrhofer, *J. Electrochem. Soc.* **2014**, *161*, H822-H830; b) X. X. Xu, A. Makaraviciute, J. Pettersson, S. L. Zhang, L. Nyholm, Z. Zhang, *Sens. Actuator B-Chem.* **2019**, *283*, 146-153.

[22] a) K. Engelsmann, W. J. Lorenz, E. Schmidt, *J. Electroanal. Chem.* **1980**, *114*, 1-10; b) K. Engelsmann, W. J. Lorenz, E. Schmidt, *J. Electroanal. Chem.* **1980**, *114*, 11-24.

[23] a) R. Adzic, E. Yeager, B. D. Cahan, *J. Electrochem. Soc.* **1974**, *121*, 474-484; b) J. Horkans, B. D. Cahan, E. Yeager, *J. Electrochem. Soc.* **1975**, *122*, 1585-1589.

[24] a) I. Ruff, V. J. Friedrich, K. Demeter, K. Csillag, *J. Phys. Chem.* **1971**, *75*, 3303–3309; b) C. Amatore, A.I. Oleinick, O.V. Klymenko, I. Svir, *ChemPhysChem* **2009**, *10*, 1586–1593; c) C. Amatore, J.-M. Savéant, D. Tessier, *J. Electroanal. Chem.* **1983**, *146*, 39-51; d) H. Brune, *Surf. Sci. Rep.* **1998**, *31*, 121-229; e) E. G. Seebauer, C. E. Allen, *Prog. Surf. Sci.* **1995**, *49*, 265-330; f) A. Vonoertzen, H. H. Rotermund, S. Nettesheim, *Surf. Sci.* **1994**, *311*, 322-330; g) R. Gomer, *Rep. Prog. Phys.* **1990**, *53*, 917-1002.

[25] a) Bard, A. J.; Faulkner, L. R., Electrochemical Methods Fundamentals and Applications; 2nd ed.; John Wiley & Sons, New York, **2001**; b) R. S. Nicholson, I. Shain, *Anal. Chem*.**1964**,*36*, 706-723; c).W.-J. Liu, B.-L. Wu, C.-S. Cha, *Russ. J. Electrochem.* **2000**, *36*, 846-851.